RESEARCH REVIEW JOURNALS
Volume-03
Issue-02
February-2018

ISSN: 2455-3085 (Online)
RESEARCH REVIEW International Journal of Multidisciplinary
www.rrjournals.com [UGC Listed Journal]

Study of Radio Wave Propagation for ISM 2.4 GHz

Priyaranjan

Research Scholar, Dept. of Physics, J.P. University, chapra

ARTICLE DETAILS

Article History
Published Online: 28 February 2018

Keywords
Radio, ISM, Propagation

ABSTRACT

This paper presents the radio channel characterization for ISM 2.4 GHz Wireless Sensor Networks (WSNs) in an inhomogeneous vegetation environment has been analyzed. This analysis allows designing environment monitoring tools based on ZigBee and WiFi where WSN and smartphones cooperate, providing rich and customized monitoring information to users in a friendly manner.

1. Introduction

When designing any wireless network a relevant aspect to be considered is the maximum distance between two nodes that still ensures a reliable wireless connection. This depends on a variety of parameters such as the transmitter power, the receiver sensitivity, the signal propagation environment, the signal frequency and the parameters of the antennas. Especially, in vegetation environments, the appearance of the foliage in the path of the communication link plays a key role on the quality of service (QoS) for wireless communications systems [1–4]. Discrete scatterers such as randomly distributed leaves, twigs, branches and tree trunks can cause attenuation, scattering, diffraction and absorption of the radiated waves. This severely constrains the design of wireless communication systems in inhomogeneous vegetation environments. The foliage effect on the path loss, shadowing and multipath dispersion has been given considerable attention from the literature. Karaliopoulos *et al.* [1] conducted some empirical foliage loss prediction models for the studies of the isolated foliage effect on a mobile-satellite channel. Bertoni [2] mainly contributed to the studies with the influence of lines of trees along the streets. An excellent work was performed by Rogers *et al.* [3] with a semi-empirical modeling of the foliage loss for the implementation of high speed wireless systems.

The main purpose is to model the radio wave propagation adequately in order to optimize the distance between devices in an actual network deployment, which is based on user location, by means of an in-house generated application which has been tested under real conditions.

2. Ray Launching Technique and Simulation Scenario

A 3D Ray Launching (RL) algorithm has been implemented in-house based on Geometrical Optics (GO) and Geometrical Theory of Diffraction (GTD). Different applications of this algorithm can be found in the literature, like the analysis of wireless propagation in closed environments [5–8], interference analysis [9] or electromagnetic dosimetry evaluation in wireless systems [10].

RL techniques are based on identifying a single point on the wave front of the radiated wave with a ray that propagates along the space following a combination of optic and electromagnetic theories, as is illustrated in Figure 1. Each ray propagates in the space as a single optic ray. The electric field E created by an antenna with a radiated power P_{rad} with a directivity $D_t(\theta_t,\Phi_t)$ and polarization ratio ($X^{\perp}$, $X^{\parallel}$) at a distance r in the free space is calculated by [11]:

$$E_i^{\perp} = \sqrt{\frac{P_{rad} D_t(\theta_t, \emptyset_t)\eta_0}{2\Pi}} \frac{e^{-j\beta_0 r}}{r} \mathrm{X}^{\perp} L^{\perp} \quad (1)$$

$$E_i^{\parallel} = \sqrt{\frac{P_{rad} D_t(\theta_t, \emptyset_t)\eta_0}{2\Pi}} \frac{e^{-j\beta_0 r}}{r} \mathrm{X}^{\parallel} L^{\parallel} \quad (2)$$

where $\beta_0 = 2\pi f_c \sqrt{\varepsilon_0 \mu_0}$, $\varepsilon_0 = 8.854 \times 10{-}12$, $\mu_0 = 4\pi \times 10{-}7$ and $\eta_0 = 120\pi$. $L^{\perp\parallel}$ are the path loss coefficients for each polarization.

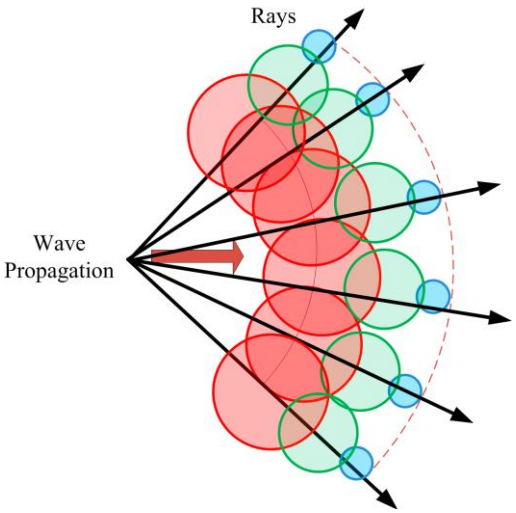

Figure 1. Wavefront propagation with rays associated with single wave front points.

When this ray finds an object in its path, two new rays are created: a reflected ray and a transmitted ray. These rays have new angles provided by Snell's law [12]. The diffracted field is calculated by [13]:

$$E_{UTD} = e_0 \frac{e^{-jks_1}}{s_1} D^{\perp\parallel} \sqrt{\frac{s_1}{s_2(s_1+s_2)}} e^{-jks_2} \quad (3)$$

where s_1, s_2 are the distances from the source to the edge and from the edge to the receiver point, respectively. $D^{\perp\parallel}$ are the diffraction coefficients given by [13, 14].

The rays considered in GO are only direct, reflected and refracted rays, leading to the existence of abrupt areas, corresponding to the boundaries of the regions where these rays exist. In order to enhance the GO approximation, the diffracted rays are introduced with the GTD and its uniform extension, the Uniform GTD (UTD). The purpose of these rays is to remove the field discontinuities and to introduce proper field corrections, especially in the zero-field regions predicted by GO. Ray launching is performed three-dimensionally, with angular resolution (horizontal and vertical planes) in a predefined solid angle that takes into account the radiation diagram of the transceivers sources. Spatial resolution when computing ray interaction is given by a uniform hexahedral mesh with cuboids of a given lateral dimension. A finite sample of the possible directions of the propagation from the transmitter is chosen and a ray is launched for each such direction.

A view of the complete schematic vegetation model developed for simulation is depicted in Figure 2 with the position of the transmitter. All the material properties for all the elements within the scenario have been considered, given the dielectric constant and the loss tangent at the frequency range of operation of the system under analysis. Due to the continuous changes of the considered environment because of the weather, it is relevant to consider different conditions for the material properties of the trees. The top portion of the tree exhibits high variability depending on the season; for example in winter, there is little foliage whereas in summer the vast totality of the volume of the top of the trees is foliage. In addition, the humidity of the wood of the trunk of the trees strongly varies depending on the weather. This has led us to consider maximum and minimum conditions for the material properties of the foliage and the trunk of the trees. For that purpose, the values obtained in [15] for the material properties of the wood and the foliage have been used. The dielectric constant and conductivity of the wood of the ash tree, which are the trees of the considered scenario is variable with the temperature, as it is shown in Equations (4) and (5) with the parameter *t*, and the dielectric constant and conductivity of the foliage of the trees is variable with humidity, as shown in Equations (6) and (7) with the parameter *h*:

$$\varepsilon_r \text{ ash wood} = -4*10^{-6}t^3 + 0.0002t^2 - 0.0212t + 21.483 \quad (4)$$

$$\sigma \text{ ash wood} = 3*10^{-7}t^3 - 0.0003t^2 - 0.004t + 7.3234 \quad (5)$$

$$\varepsilon_r \text{ folige} = 137h^3 - 69.688h^2 + 23.385h + 1.4984 \quad (6)$$

$$\sigma \text{ foliage} = 1.1541h^3 - 0.5489h^2 + 0.1669h - 0.0004 \quad (7)$$

To set up the dielectric constant and conductivity of the ash wood and the foliage, thresholds for the maximum and minimum humidity and temperature have been considered. These values have been fixed in the interval (0%, 30%) for the humidity and (20°, 40°) for the temperature, according to [15].

Simulations have been performed for the minimum, medium and maximum values and the results shown in this work correspond with the medium values for the humidity and temperature.

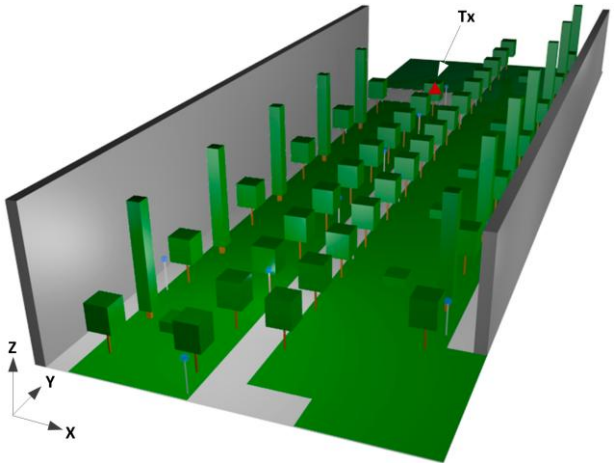

Figure 2. Schematic vegetation environment for simulation in the 3D Ray Launching algorithm.

The material parameters used in the simulation are defined in Table 1 [16, 17].

Table 1. Material properties in the ray launching simulation.

Parameter	Permittivity (ε_r)	Conductivity (σ) [S/m]
Air	1	0
Concrete	5.66	0.142
Grass	30	0.01
Trunk tree	Equation (4)	Equation (5)
Tree foliage	Equation (6)	Equation (7)

For the simulations, an antenna has been placed at the point (X = 11.95 m, Y = 70.8, Z = 1.2), depicted with a red triangle in Figure 2. The radiating element is a wireless ZigBee mote which has been configured as a dipole, transmitting 18 dBm at 2.41 GHz. Simulation parameters are shown in Table 2.

Table 2. Parameters in the ray launching simulation.

Frequency		2.41 GHz
Vertical plane angle resolution	Δθ	0.5°
Horizontal plane angle resolution	Δφ	0.5°
Reflections		6
Transmitter Power		18 dBm
Cuboids resolution		0.5 m

3. Simulation Results

Once the simulation scenario has been defined, simulation results can be obtained. Figure 3 shows the power distribution within the considered scenario for different heights. As it can be seen, the influence of the obstacles (like the trees and streetlights) can be easily appreciated. It is shown that the morphology as well as the topology of the considered scenario has a noticeable impact on radio wave propagation.

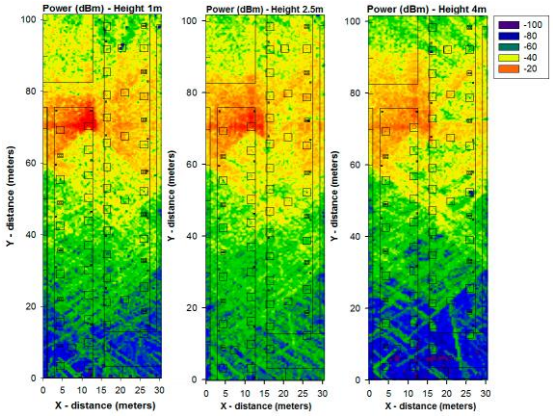

(a)

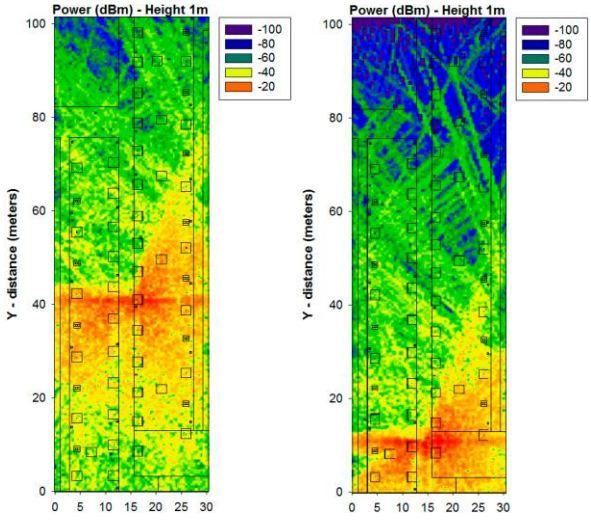

(b)

Figure 3. Estimation of received power (dBm) on the vegetation environment obtained by the 3D Ray Launching algorithm (**a**) For the transmitter antenna placed at a fixed point and for different heights (**b**) For two different points of the transmitter antenna for the same height.

In order to gain insight into the influence of the scenario in radio wave propagation, different locations of the transmitter antenna has been considered. Figure 5b represents the received power for 1 m height for two different points (X = 14.7 m, Y = 41, Z = 1.2) and (X = 14.7 m, Y = 11, Z = 1.2). It is shown that the position of the transmitter antenna plays a key role in the distribution of the received power, because electromagnetic phenomena, such as reflections, diffraction and absorption due to obstacles are different depending of the environment. Therefore, this change in the overall signal levels obtained can provide with mean values of received signal but the consideration of local point values requires analysis for the specific transceivers positions employed.

Figure 4 depicts a linear distribution from within the transmitter-receiver range of power along the Y-axis of the considered scenario, for two different values of X, for different heights. It is observed that the distribution of power exhibits large variability due mainly to the strong influence of multipath components.

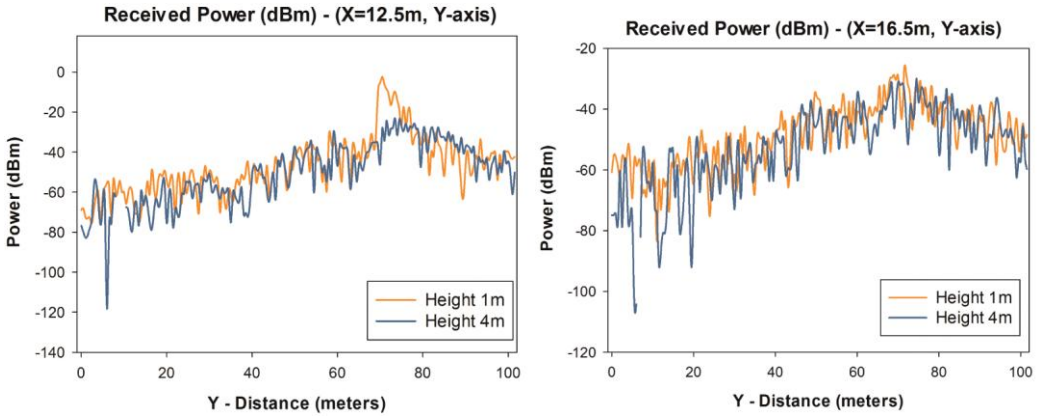

Figure 4. Estimation of radials of received power (dBm) along the Y-axis for X = 12.5m and X = 16.5 m for different heights.

An important radioelectric phenomenon in this type of environment is given by multipath propagation. To illustrate this fact, the power delay profile for the central location of the scenario has been obtained and it is shown in Figure 5. As it is observed, there are several echoes in the scenario inherent to the behavior of multipath channels.

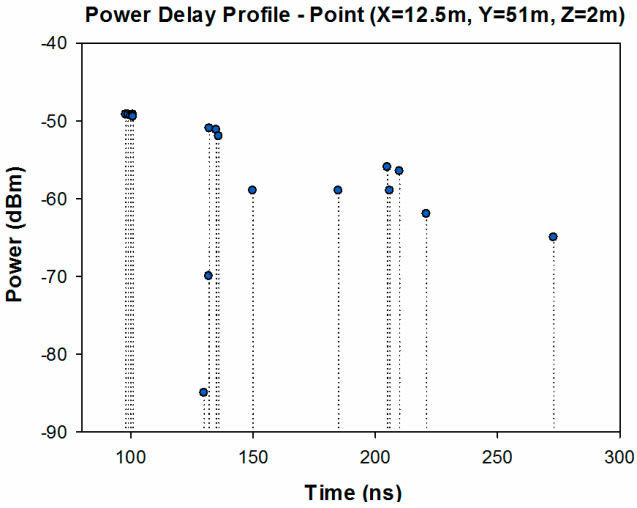

Figure 4. Power Delay Profile at a given cuboid, located at the central location in the considered scenario.

Time dispersion varies widely in a mobile radio channel depending on the geometrical position relationships among the transmitter, the receiver and the surrounding physical environment.

4. Experimental Setup

ZigBee technology has been chosen for emulating a WSN. Specifically, the wireless devices used for the measurements have been the XBee Pro motes from Digi International Inc. These wireless communication devices operate in the unlicensed ISM 2.4 GHz band and the whip antenna mounted on it has an omnidirectional diagram with a gain of 1.5 dBi, which has been taken into account to calibrate the measured values. For transmitting or processing received data, the motes have been connected to a PC via USB cable after being plugged into an XBee explorer unit.

The measurement results for received power can be seen in Figure 5, where 3D ray launching simulation results have also been included for comparison.

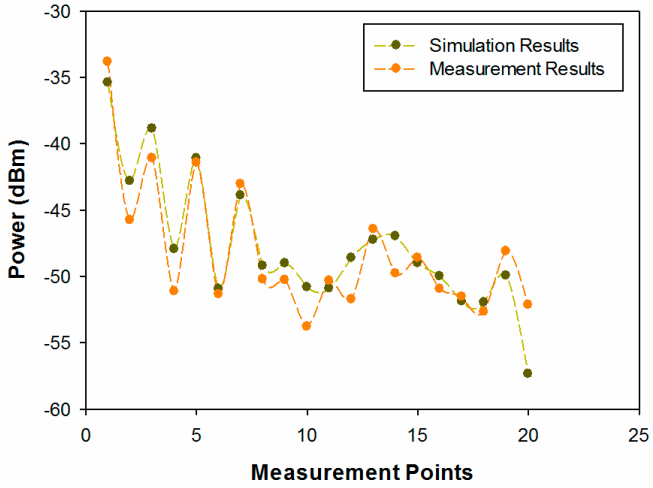

Figure 5. Comparison of simulation *vs.* measurements.

Good agreement is observed between the simulation results and the measurements. The resulting error mean for those measurement points is 1.67 dB, a low error that indicates that the proposed in-house 3D ray launching simulation method works properly, validating in the same way the simulation results shown in the previous sections of this work. Once the received power level for different positions within the vegetation environment has been measured and the simulation method has been validated, the second measurement campaign has been performed. The aim of these measurements is to deepen the analysis of the radio propagation in a highly complex environment such as the considered scenario.

5. Conclusions

In this work, a detailed characterization and analysis of the radio wave propagation for ISM 2.4 GHz wireless sensor networks in heterogeneous vegetation scenarios allow to design environment monitoring tools based on ZigBee and WiFi technologies where WSN and smarthpones cooperate providing rich and customized monitoring information to users in a friendly manner, enabling context aware scenario implementation.

References

1. Karaliopoulos, M.S.; Pavlidou, F.N. Modelling the land mobile satellite channel: A review. *IEE Electron. Commun. Eng. J.* **1999**, *11*, 235–248.
2. Bertoni, H.L. *Radio Propagation for Modern Wireless Systems*; Prentice Hall PTR: Upper Saddle River, NJ, USA, 2000.
3. Rogers, N.C.; Seville, A.; Richter, J.; Ndzi, D.; Savage, N.; Caldeirinha, R.; Shukla, A.; Al-Nuaimi, M.O.; Craig, K.H.; Vilar, E.; *et al. A Generic Model of 1–60 GHz Radio Propagation through Vegetation*; Technical Report; UK Radiocommunications Agency: London, UK, 2002.
4. Meng, Y.S.; Lee, Y.H.; Ng, B.C. Study of propagation loss prediction in forest environment. *Prog. Electromagn. Res. B* **2009**, *17*, 117–133.

5. Azpilicueta, L.; Falcone, F.; Astráin, J.J.; Villadangos, J.; García Zuazola, I.J.; Landaluce, H.; Angulo, I.; Perallos, A. Measurement and modeling of a UHF-RFID system in a metallic closed vehicle. *Microw. Opt. Technol. Lett.* **2012**, *54*, 2126–2130.
6. Moreno, A.; Angulo, I.; Perallos, A.; Landaluce, H.; Zuazola, I.J.G.; Azpilicueta, L.; Astráin, J.J.; Falcone, F.; Villadangos, J. IVAN: Intelligent Van for the Distribution of Pharmaceutical Drugs. *Sensors* **2012**, *12*, 6587–6609.
7. Nazábal, J.A.; Iturri-López, P.; Azpilicueta, L.; Falcone, F.; Fernández-Valdivielso, C. Performance Analysis of IEEE 802.15.4 Compliant Wireless Devices for Heterogeneous Indoor Home Automation Environments. *Int. J. Antennas Propag.* **2012**, doi:10.1155/2012/176383.
8. Led, S.; Azpilicueta, L.; Aguirre, E.; Martínez de Espronceda, M.; Serrano, L.; Falcone, F. Analysis and Description of HOLTIN Service Provision for AECG monitoring in Complex Indoor Environments. *Sensors* **2013**, *13*, 4947–4960.
9. Iturri, P.L.; Nazábal, J.A.; Azpilicueta, L.; Rodriguez, P.; Beruete, M.; Fernández-Valdivielso, C.; Falcone, F. Impact of High Power Interference Sources in Planning and Deployment of Wireless Sensor Networks and Devices in the 2.4 GHz frequency band in Heterogeneous Environments. *Sensors* **2012**, *12*, 15689–15708.
10. Aguirre, E.; Arpón, J.; Azpilicueta, L.; de Miguel, S.; Ramos, V.; Falcone, F. Evaluation of electromagnetic dosimetry of wireless systems in complex indoor scenarios within body human interaction. *Prog. Electromagn. Res. B* **2012**, *43*, 189–209.
11. Cardama, A. *Antenas*; Editions Universitat Politécnica de Catalunya: Barcelona, Spain, 1993.
12. Hristov, H.D. *Fresnel Zones in Wireless Links, Zone Plate Lenses and Antennas*; Artech House, Inc.: 685 Canton Street, Norwood, MA, USA, 2000.
13. Luebbers, R.J. A Heuristic UTD Slope Diffraction Coefficient for Rough Lossy Wedges. *IEEE Trans. Antennas Propag.* **1989**, *37*, 206–211.
14. Luebbers, R.J. Comparison of Lossy Wedge Diffraction Coefficients with Application to Mixed Path Propagation Loss Prediction. *IEEE Trans. Antennas Propag.* **1988**, *36*, 1031–1034.
15. Vyacheslav, V. Komarov. *Handbook of Dielectric and Thermal Properties of Materials at Microwave Frequencies*; Artech House, Inc.: 685 Canton Street, Norwood, MA, USA, 2012.
16. Balanis, C.A. *Advanced Engineering Electromagnetics*. Wiley: New York, NY, USA, 1989; Volume 205.
17. Cuiñas, I.; García Sánchez, M. Permittivity and conductivity measurements of building materials at 5.8 GHz and 41.5 GHz. *Wirel. Pers. Commun.* **2002**, *20*, 93–100.

